FEBS Letters 581 (2007) 3051–3056

Effects of pH and salt concentration on the siRNA binding activity of the RNA silencing suppressor protein p19

Roger Koukiekolo[a], Selena M. Sagan[a,b], John Paul Pezacki[a,b,c,*]

[a] The Steacie Institute for Molecular Sciences, National Research Council of Canada, 100 Sussex Dr. Ottawa, Canada K1A 0R6
[b] Department of Biochemistry, Microbiology and Immunology, Ottawa Institute of Systems Biology, University of Ottawa, Health Sciences Campus, 451 Smyth Road, Ottawa, Canada K1H 8M5
[c] Department of Chemistry, University of Ottawa, 10 Marie-Curie, Ottawa, Canada K1N 6N5

Received 5 April 2007; revised 17 May 2007; accepted 18 May 2007

Available online 4 June 2007

Edited by Shou-Wei Ding

Abstract **The RNA silencing pathway is an important component of the anti-viral immune response in eukaryotes, particularly in plants. In turn, many viruses have evolved mechanisms to evade or suppress this pathway. Tombusviruses such as the Carnation Italian ringspot virus (CIRV) express a 19 kDa protein (p19) that is a suppressor of RNA silencing in infected plants. This protein acts as a dimer and binds specifically to short-interfering RNA (siRNA) through electrostatic interactions between charged residues in the binding cleft. Since pH and salt concentrations can vary widely from host to host, we have investigated the influence of these parameters on the siRNA binding activity of CIRV p19. Previously, we established a convenient fluorescence-based method for assaying CIRV p19:siRNA binding using Ni^{2+}–NTA coated 96-well plates. Using this method, we observe that the CIRV p19 protein binds to siRNA with nanomolar affinity and that this binding is sensitive to pH and salt concentration. The pH-dissociation constant profile shows that CIRV p19:siRNA binding is dependent on three different apparent pK_a values. The values extrapolated from the curve are 7.1, 8.0 and 10.6 that we interpret as the ionization of one or more histidine, cysteine and lysine residues, respectively. We find that the optimal suppression of RNA silencing by CIRV p19 occurs in the pH range from 6.2 to 7.6.**

Keywords: Suppressors of RNA silencing; Tombusviruses; pH-dependence; RNA–protein interactions

1. Introduction

The dsRNA response in plant cells is a critical component of the anti-viral immune response to RNA viruses [1–3]. One component of the double-stranded RNA (dsRNA) response is the evolutionarily conserved RNA silencing pathway, involving the biogenesis of short interfering RNAs (siRNA) molecules [4–8]. The siRNAs are assembled into an RNA-induced silencing complex (RISC) and guide the degradation of single-stranded complementary viral RNA [2,9]. As a result, many plant viruses have adopted strategies for evading or directly suppressing the host cell's RNA silencing pathway [1,3,10]. Tombusviruses have adapted to the RNA silencing pathway through the production of a 19 kDa protein (p19) that acts as an siRNA inhibitor [4,10–14] and reviewed in [15]. The p19 protein acts as a dimer and binds to the minor groove of siRNA duplexes [12,13]. It binds size selectively to 21–25 nt siRNA with high affinity (nM–pM range) and little sequence-specificity [12,13], although some preference towards siRNAs with high GC content have been observed [16]. The p19 protein forms a tail-to-tail homodimer through hydrogen bonding, hydrophobic and salt bridge interactions [12,13]. The p19 dimer appears to block silencing by directly binding siRNA and sequestering it from the RNA silencing pathway machinery [1,12,13,17].

The molecular basis for p19 binding to siRNA has been revealed in the recent crystal structures of p19 bound to 21-nt siRNA duplexes [12,13]. The crystal structure shows that the p19 homodimer binds the RNA duplex through basic and polar amino-acid interactions with the phosphate backbone and 2′-hydroxyl groups of the RNA. In addition, two crucial tryptophan residues (Trp^{39} and Trp^{42}) make end-capping interactions with the 5′ ends of the siRNA resulting in the stacking of exposed base pairs at the ends of the RNA duplex [12,13]. The importance of one or more cysteine residues for p19 function has also been reported recently [18].

The host plant's physiology can be greatly perturbed by environmental factors such as water levels, acidity/alkalinity, temperature, as well as variations in mineral and salt content which can affect the virulence of invading pathogens [19,20]. Changes in pH and ionic strength may specifically affect the ability of p19 to act as a suppressor of RNA silencing. Consistent with this, structural and mutational studies have indicated that interactions involving ionizable residues are critical for p19–RNA interactions [12,13,21]. Here, we report a detailed characterization of pH and ionic strength dependence on the equilibrium binding of siRNA to the high affinity binding pocket of CIRV p19 in vitro.

2. Materials and methods

2.1. Protein expression and purification

Bacterial expression of CIRV p19 His-tag (p19-H) was carried out in *E. coli* strain BL21 (DE3) cells harboring the pTriEx-p19 construct [17]

*Corresponding author. Address: The Steacie Institute for Molecular Sciences, National Research Council of Canada, 100 Sussex Dr. Ottawa, Canada K1A 0R6. Fax: +1 613 941 8447.
E-mail address: John.Pezacki@nrc-cnrc.gc.ca (J.P. Pezacki).

Abbreviations: CIRV, Carnation Italian Ringspot virus; p19, tombusvirus suppressor of RNA silencing protein with apparent molecular mass of 19 kDa; siRNA, short interfering RNAs; dsRNA, double-stranded RNA; dsRBM, double-stranded RNA-binding motif

0014-5793/$32.00
doi:10.1016/j.febslet.2007.05.064

at 37 °C until an OD_{600} of 0.5–0.6 was achieved. Expression of CIRV p19-H was induced by IPTG at a final concentration of 1 mM. Cultures were then grown for an additional 4–5 h at 30 °C. Bacterial pellets were resuspended in lysis buffer (50 mM NaH_2PO_4, 300 mM NaCl, 10 mM imidazole, 1 mg/ml lysozyme (Sigma), pH 8.0) and lysed by sonication on ice. The CIRV p19-H protein was purified from the soluble fraction of lysate by binding to a Ni^{2+}-NTA column (Pharmacia, Peapack, NJ). The resin was washed with wash buffer I (50 mM NaH_2PO_4, 500 mM NaCl, 20 mM imidazole, pH 8.0), then wash buffer II (50 mM NaH_2PO_4, 300 mM NaCl, 20% glycerol, pH 8.0), and finally with wash buffer III (50 mM NaH_2PO_4, 300 mM NaCl, 1% Tween-20, pH 8.0). Elution of CIRV p19-H was carried out with elution buffer (50 mM NaH_2PO_4, 300 mM NaCl, 250 mM imidazole, pH 8.0). The pooled eluates were desalted using the PD-10 column (Pharmacia) and concentrated into 1 ml of 50 mM Tris–HCl buffer (pH 8.0) using the Ultrafree 10-kDa membrane (Millipore, Concord, MA).

2.2. Fluorescence detection assays

Binding assays on purified CIRV p19-H were performed using the fluorescent siRNA Cy3-CSK-2 (5′-Cy3-CUACCGCAUCAUGUACCAUdTdT-3′), as described previously [18]. Duplex siRNAs were purchased from Dharmacon (Lafayette, CO). The dissociation constants were assessed by fluorescence detection assays carried out using 96-well Ni^{2+}–NTA plates (Qiagen Inc., Mississauga, Ontario) as described previously [18]. Before studying the effects of pH on the activity of p19, the stability of the protein bound to the Ni^{2+}–NTA matrix under conditions of varying pH was examined by incubating the 96-well Ni^{2+}-NTA plates with 200 μl of appropriate buffer solutions with pH ranging from 6.0 to 12.0. After a 3 h incubation period, the buffer solutions were removed and replaced with 200 μl of CIRV p19-H (10 μg/ml) in binding buffer (50 mM PBS–BSA, pH 7.2) for a 2 h immobilization. After three washes, 100 nM of Cy3-CSK-2 siRNA in binding buffer was added to each well. After a 1 h incubation period, plates were washed three times and the relative fluorescence intensity was assessed by measuring fluorescence at E_x = 546 nm and E_m = 590 nm using a Spectramax M2 Plate Reader (Molecular Devices Corporation, Sunnyvale, CA). The relative fluorescence intensity was similar for all wells, confirming the stability of the Ni^{2+}–NTA under varying pH and buffer conditions.

With respect to binding specificity, a small peptide (~12-kDa) [18] containing an 8× His-tag at its C-terminus (peptide-H) was expressed and purified as described above for CIRV p19-H. Purified CIRV p19-H or peptide-H (200 μl, 10 μg/ml) in 1× PBS, 0.2% BSA, pH 7.2 were pre-bound to the surface of each well of Ni^{2+}–NTA plates for 3 h at room temperature. Wells were then washed twice with wash buffer (1× PBS containing 0.05% Tween 20 and 1 mM EDTA). Two-hundred microliters of 1× PBS 0.2% BSA, pH 7.2 was then placed in each well and the background fluorescence (E_x = 546 nm and E_m = 590 nm) was measured with a Spectramax M2 Plate Reader (Molecular Devices Corporation) for normalization purposes. The wells were then washed once more with wash buffer before addition of the siRNAs. The Cy3-labeled siRNAs (0–4 μM, diluted in buffers with appropriate pH) were then added to each well and incubated in the dark for 1 h at room temperature. Wells were then washed three times with wash buffer and 200 μl of 1× PBS, 0.2% BSA, pH 7.2 was placed into each well for fluorescence measurement. Fluorescence detection of bound Cy3-labeled siRNAs (E_x = 546 nm and E_m = 590 nm) was measured with a Spectramax M2 Plate Reader (Molecular Devices Corporation). The relative fluorescence of specific binding was calculated by subtracting the fluorescence values obtained from siRNA binding to peptide-H from the fluorescence values of siRNA binding to CIRV p19-H. For ionic strength experiments, following the immobilization of CIRV p19-H, the siRNA (0–4 μM) was diluted in 1× PBS 0.2% BSA containing either NaCl, $NaClO_4$, or NH_4F of the appropriate concentration (up to 1 M) was added to the immobilized CIRV p19-H. The measurements were performed as described above.

2.3. pH-binding profiles

The influence of pH on the siRNA binding activity of CIRV p19-H was determined by monitoring siRNA binding in fluorescence detection assays carried out over the pH range from 6.0 to 12.0. In order to determine the dissociation constants for CIRV p19-H binding to a model 21-nt siRNA, aliquots of the 5′-Cy3-labeled siRNA were added at increasing concentrations to 96-well Ni^{2+}-NTA coated plates containing bound CIRV p19-H as described previously [18]. The fluorescent siRNA remaining bound to CIRV p19-H was measured after a 1 h incubation period. The fraction of bound 5′-Cy3-labeled siRNA was calculated by determining the fraction of the original fluorescence intensity that remained after removal of the unbound 5′-Cy3-labeled siRNA. The fluorescence data were fit to Eq. (1) in order to determine the equilibrium dissociation constant (K_d) values for CIRV p19:siRNA binding.

$$f = [\mathrm{siRNA}]_{\max} \cdot \left(\frac{[\mathrm{siRNA}]_U}{[\mathrm{siRNA}]_U + K_d} \right) \quad (1)$$

where f denotes the relative fluorescence intensity which is directly proportional to the fractional occupancy of p19; $[\mathrm{siRNA}]_{\max}$ denotes the maximal binding of siRNA; $[\mathrm{siRNA}]_U$, the fraction of unbound siRNA; and K_d, the equilibrium dissociation constant.

Data for the log K_d vs. pH profile was fit to an equation that represents the titration of three pK_a values, as shown in:

$$\log(K_d'^{\mathrm{pH}}) = \frac{\mathrm{Limit}_1 + \mathrm{Limit}_2 \times 10^{(\mathrm{pH}-\mathrm{p}K_{a1})}}{10^{(\mathrm{pH}-\mathrm{p}K_{a1})} + 1} - \frac{\mathrm{Limit}_2 - \mathrm{Limit}_3 \times 10^{(\mathrm{pH}-\mathrm{p}K_{a2})}}{10^{(\mathrm{pH}-\mathrm{p}K_{a2})} + 1} - \frac{\mathrm{Limit}_3 - \mathrm{Limit}_4 \times 10^{(\mathrm{pH}-\mathrm{p}K_{a3})}}{10^{(\mathrm{pH}-\mathrm{p}K_{a3})} + 1} \quad (2)$$

2.4. Buffer composition

The design and preparation of buffers of varying pH were prepared using a recipe calculator for thermodynamically correct buffers, R. Beynon from the University of Liverpool (Website: http://liv.ac.uk/buffers/buffercalc.html). All buffers were prepared at an ionic strength of 0.1 M (NaCl). In addition, all buffers were prepared and used at ambient temperature (25 °C) and constant ionic strength.

2.5. Graphs and data analysis

All graph analyses were performed using the Graph-Pad Prism® computer program (GraphPad Software Inc., San Diego, CA, USA) or GraFit version 4.0 (Erithacus Software Ltd., Surrey, UK).

3. Results

3.1. Effect of pH on the siRNA binding activity of p19

The effect of pH and the extent of changes in protonation state of p19 in the CIRV p19-H:siRNA interaction was determined using fluorescence detection assays. The dissociation constants for CIRV p19-H:siRNA binding, obtained from fluorescence detection assays, under a range of pH and buffer conditions are summarized in Table 1. Representative binding curves plotted as the relative fluorescence intensity vs. the concentration of the 5′-Cy3-labeled 21-nt siRNA over a range of pH values from 6.1 to 12.0 is shown Fig. 1A. We observed that the CIRV p19-H:siRNA interaction was highly affected by changes in pH (Fig. 1A). We also plotted of the log K_d vs. pH (Fig. 1B). This data were fit to an equation that represents the titration of three pK_a values (Eq. (2), described in Section 2). The pK_a values extrapolated from the curve correspond to 7.1, 8.0 and 10.6. We interpret these values as the ionization of one or more histidine, cysteine and lysine residues, respectively.

From the binding data described in Table 1 and Fig. 1, we find that CIRV p19-H is able to bind siRNA efficiently over a wide range of pH values spanning from 6.1 to 9.0. Relatively tight binding to siRNA was observed at low pH (K_d = 136.7 nM and 112.1 nM, at pH 6.1 and 6.2, respectively), whereas the binding was reduced as much as 4.7-fold with an increase in pH from 6.7 to 10.5, and binding of siRNA

Table 1
Dissociation constants for CIRV p19-H:siRNA binding under a range of pH and buffer conditions[a]

pH	Ionic strength (salt) (M)	Buffer	K'_d (nM)
5.9	0.1 (NaCl)	Pyridine	211
6.1	0.1 (NaCl)	Pyridine	137
6.2	0.1 (NaCl)	NaH_2PO_4	112
6.7	0.1 (NaCl)	NaH_2PO_4	199
7	0.1 (NaCl)	NaH_2PO_4	239
7.2	0.1 (NaCl)	NaH_2PO_4	513
7.2	0.2 (NaCl)	NaH_2PO_4	600
7.2	0.35 (NaCl)	NaH_2PO_4	1100
7.2	0.6 (NaCl)	NaH_2PO_4	~3100
7.2	0.85 (NaCl)	NaH_2PO_4	~5800
7.2	1.1 (NaCl)	NaH_2PO_4	~7200
7.2	0.1 ($NaClO_4$)	NaH_2PO_4	580
7.2	0.15 ($NaClO_4$)	NaH_2PO_4	720
7.2	0.35 ($NaClO_4$)	NaH_2PO_4	702
7.2	0.6 ($NaClO_4$)	NaH_2PO_4	~18000
7.5	0.1 (NaCl)	NaH_2PO_4	323
7.7	0.1 (NaCl)	NaH_2PO_4	315
7.9	0.1 (NaCl)	NaH_2PO_4	440
8	0.1 (NaCl)	NaH_2PO_4	271
8.1	0.1 (NaCl)	NaH_2PO_4	436
8.6	0.1 (NaCl)	Tris	207
9	0.1 (NaCl)	Tris	240
9.4	0.1 (NaCl)	Ethanolamine	213
9.9	0.1 (NaCl)	Ethanolamine	295
10.2	0.1 (NaCl)	Ethanolamine	430
10.5	0.1 (NaCl)	Ethanolamine	531
11	0.1 (NaCl)	Piperidine	~2480
12	0.1 (NaCl)	Piperidine	~3960

[a] K_d is the dissociation constant measured by fluorescence in CIRV-p19 array binding assays.

dropped off dramatically above pH 11 (>22-fold). We observed that the deprotonation of a residue in CIRV p19-H with the apparent pK_a of 7.1 increases the K_d of CIRV p19-H for siRNA. In addition, the deprotonation of a residue in CIRV p19-H with an apparent pK_a of 8.0 decreases the K_d value, indicating that this change in ionization state is favorable for siRNA binding activity. Finally, the deprotonation of a residue in CIRV p19-H with an apparent pK_a of 10.6 obliterates siRNA binding activity. As described in structural studies of CIRV p19 and the homologous TBSV p19, the high affinity of p19 for siRNA is a result of interactions with the negatively-charged phosphate backbone of the RNA duplex with specific charged residues located in the binding pocket of the p19 dimer [12,13]. The pH-dependent changes in siRNA binding activity likely result from the protonation/deprotonation of one or more of these positively-charged residues.

In addition to the effect of pH on siRNA binding activity, we also assessed the reversibility of pH-dependent binding of CIRV p19-H to siRNA. Stability measurements were conducted by measuring the relative fluorescence of the CIRV p19-H:siRNA interaction across a broad range of pH values. Purified CIRV p19-H was incubated at various pH values ranging from 6.2 to 12.0 for 1 h. The siRNA binding activity of CIRV p19-H was then assayed in buffer containing a single, saturating concentration of siRNA (1 μM siRNA, in 1× PBS, pH 7.0). We observed comparable siRNA binding activity at each pH value tested (data not shown). This indicates that the pH-dependence of the CIRV p19-H:siRNA interaction is reversible and is therefore likely due to a reversible changes in the ionization state of the side chains of key amino acid residues within the p19 protein.

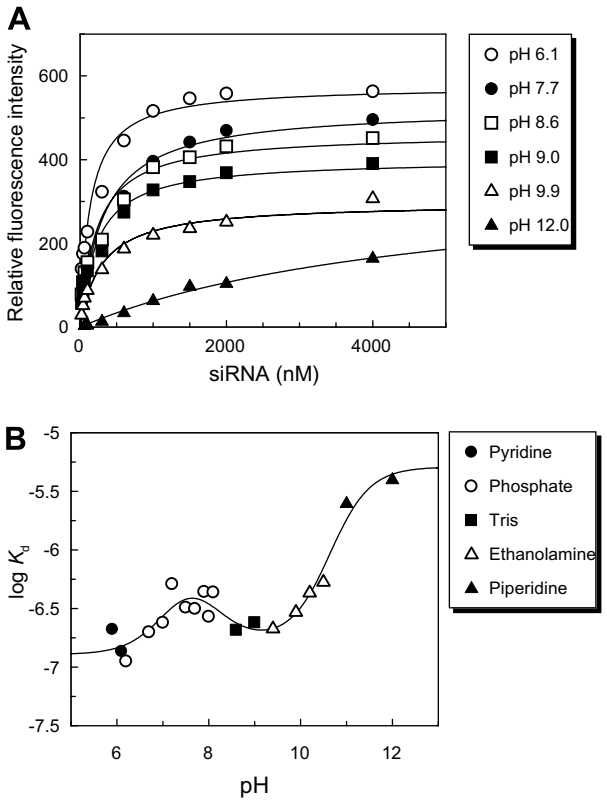

Fig. 1. Effect of pH on CIRV p19-H binding to siRNA. (A) Representative overlayed plots of siRNA binding of CIRV p19-H across a broad pH range. (B) log K_d plotted as a function of the pH. In all siRNA binding experiments the ionic strength was maintained at 100 mM with NaCl. Data points represent the average measurement values from triplicate experiments with standard errors ranging from 10% to 20%. Best-fit binding hyperboles are shown with the assumption that one CIRV p19-H dimer binds to a single siRNA duplex. All experiments were conducted with the same batch of plates and protein stock solutions to ensure that the saturation point for each well would be the same within experimental error.

3.2. Electrostatic effects on the dissociation constant for p19

To determine the relative contribution of electrostatic forces in siRNA binding activity, the equilibrium dissociation constant of p19 binding to siRNA was characterized in a series of experiments at differing ionic strengths. This was carried out by varying the concentration of NaCl from 0.1 to 1.0 M. The resultant binding curves demonstrate that the CIRV p19-H:siRNA interaction is highly dependent on NaCl concentration (Fig. 2). We observed a decrease in the affinity of p19 for siRNA (K_d ranging from 600 nM to ~10 μM) when the NaCl concentration was increased from 0.1 M to 1.0 M, respectively. While the siRNA binding activity was only slightly affected in the presence of 0.25 M NaCl (1.8-fold), a very pronounced inhibition of siRNA binding (>10-fold) was observed by increasing the concentration to 0.75 M NaCl. The siRNA binding activity of CIRV p19-H was almost completely inhibited when the concentration was increased to 1.0 M NaCl (Fig. 2).

3.3. Anion effect on CIRV p19-H:siRNA binding

In order to study the effect of ionic strength in more detail, we evaluated the anionic effect of $NaClO_4$ on CIRV p19-H:siRNA binding. The historical use of sodium perchlorate

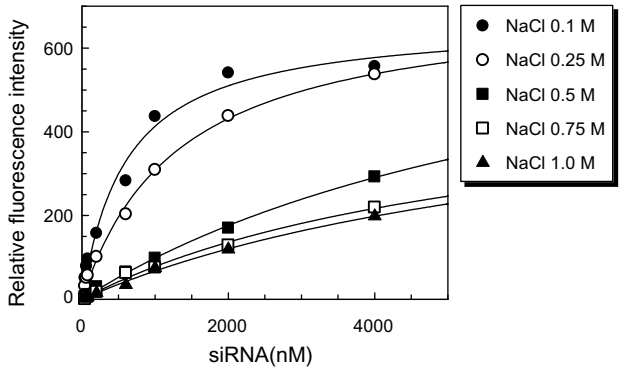

Fig. 2. Effect of NaCl on CIRV p19-H:siRNA interactions. Representative plots of siRNA binding for CIRV p19-H at various concentrations of NaCl, pH 7.2. The curves are best fit by non-linear regression to one site model described in Eq. (1).

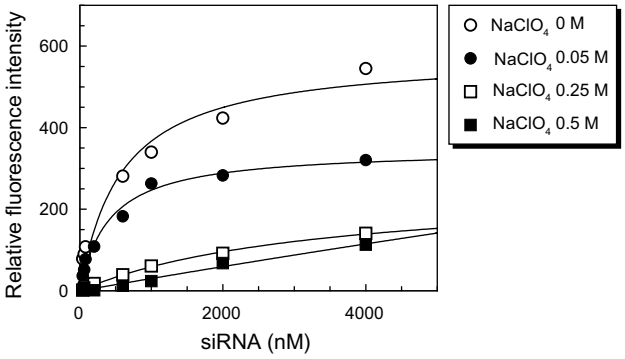

Fig. 3. Effect of $NaClO_4$ on CIRV p19-H:siRNA interactions. Representative plots of siRNA binding for CIRV p19-H at various concentrations of $NaClO_4$, pH 7.2. The curves are best fit by non-linear regression to one site model described in Eq. (1).

as an anionic hydrophilic ion-pairing reagent has been used for its ability to suppress non-specific ionic interactions between positively-charged residues and any negatively charged residues. The binding curves shown in Fig. 3 show a strong salt effect of $NaClO_4$ on CIRV p19-H:siRNA interactions. We observed that at equal concentrations (0.25 M and 0.5 M), Cl^- showed a smaller inhibition of siRNA binding (50% and 80%, respectively) when compared to the larger effects observed from the ClO_4^- salt (92% and 97%, respectively). The more pronounced response obtained with ClO_4^- is consistent with the salt effects for p19:siRNA binding following the Hofmeister series [22,23]. In addition, we tested the effects of the F^- anion using the salt NH_4F. The effect of F^- was smaller than that of the Cl^- salt (NH_4F reduced the binding by only ~25% at 1.0 M salt compared with a corresponding 75% reduction in the presence of 1.0 M NaCl) which is also consistent with the Hofmeister series (data not shown).

4. Discussion

Molecular recognition of RNA is a key event for numerous biological pathways including transcription, trafficking, editing, maturation of cellular RNA as well as RNA interference [24]. The biochemical and biophysical parameters that govern these key events are common to p19:siRNA interactions. Many proteins including RNA-dependent protein kinase PKR, spliceosomal U1A protein, *Drosophila* Staufen protein, Dicer or RNase III have been shown to bind specific dsRNA targets owing to their dsRNA-binding motifs (dsRBM) [25–28]. Of the proteins that are known to bind to dsRNA, most utilize RNA structures such as loops, bulges and mismatches, as well as direct specific contacts of surface residues for dsRNA recognition. Owing to the strong negative electrostatic field associated with the RNA phosphate backbone, charged interactions are likely to be important for proper RNA binding [29,30]. Indeed, hydrogen bonds and electrostatic interactions are commonly involved in RNA–protein complexes. Mutagenesis and NMR studies of the Staufen protein have demonstrated that the electrostatic interaction mediated by basic residues plays an important role in dsRBM–RNA interaction [31]. The well-characterized U1A/U1 small nuclear ribonucleoprotein complex provides the role of electrostatic interaction in the contribution of the energy needed in protein–RNA interaction [32]. Two structure-based studies, on dsRNA processing by dicer [25] and the PAZ domain of the human Argonaute 2 protein bound to siRNA [33,34], also demonstrate the impact of hydrogen bonds and electrostatic interactions on dsRNA binding activity.

CIRV p19 interacts with siRNA over the entire length of the molecule through hydrogen-bonds, electrostatic and end-capping interactions [12,13]. Here, we investigated the pH-dependence and salt effects pertaining to the CIRV p19:siRNA binding interaction. Our results indicate that, depending on their location, key basic amino-acids are important in CIRV p19 contacting the RNA and they are also likely to help stabilize the CIRV p19:siRNA complex. Between pH 6 and 7 the binding capacity is maximal; however, outside this pH range, the p19 protein's ability to bind 21-nt siRNA decreases. The dissociation constant curve as a function of pH (Fig. 1B) suggests that the CIRV p19:siRNA interaction can be affected by at least three electrostatic groups (pK_a of 7.1, 8.6 and 10.5) that are titrated between pH 6 and 12. The pH effect is assumed to be electrostatic in nature due to non-specific repulsions that arise when the protein is highly charged [35–37]. The observed pH-dependent binding behavior might be the result of the overall affect on structural stability and/or the result of titrations of amino acid side chains that are directly involved in binding to the siRNA. The theoretical isoelectric point (pI) of CIRV p19 is 5.9. This value does not correspond to any of the observed pK_a values extrapolated from Fig. 1B. The much higher value obtained can be explained by the fact that for some proteins, the pH of maximum stability does not coincide with the isoelectric pH but can be accounted for by the burial in hydrocarbon core of some titratable groups [35]. The first observed pK_a does not appear to correspond to any of the side chains known to be directly involved in the binding of CIRV p19 to siRNA [12]. Therefore, we hypothesize that the first observed pK_a value of 7.1 is attributably to a titratable group that influences protein stability. One possible candidate is H45, which is known to be involved in side-chain interactions that position helix H1 relative to the β-sheet core of each monomer in the p19 dimer [12].

Both the second and third observed pK_a values in the $\log K_d$ vs. pH plot in Fig. 1B can be assigned to changes in the ionization of key amino acids such as lysine and cysteine. Based on the crystal structures of CIRV p19 and the close homologue

TBSV p19 [12,13], the 21-nt siRNA interacts with basic and polar groups of p19 that bind the phosphate backbone (R11, R18, R43, R115, T40, K60, K67, K71, S62, S113, S120, W42 and Q107). Mutations of K60 and K71 (conserved among tombusviruses) of TBSV p19 lead to decreases in the lethal necrosis phenotype [38,39]. Based on these observations, we hypothesize that the deprotonation of the lysine residues (corresponding to the pK_a titrated at 10.5 in Fig. 1B) lead to the destabilization of electrostatic interactions between p19 and the siRNA phosphate backbone and resulted in the drastic decrease in the observed dissociation constant. Moreover, the observed effect is most likely associated with the deprotonation of R11, R18 and R115. Unfortunately, we were not able to titrate the arginine residues in the binding cleft because of the lack of stability of CIRV p19 at pH values above 12. Analogously, the observed pK_a of 8.6 can be attributed to the ionization of one or more cysteine residues. Previously, we have shown that cysteine alkylation can perturb CIRV p19:siRNA binding [18]. Interestingly, the pH-binding profile suggests that deprotonation of one or more cysteine residues may be beneficial to the binding affinity of CIRV p19 for 21-nt siRNA. It is also possible that the reduced binding affinity observed at higher pH could be due to structural changes resulting from deprotonation of other amino acid side chains that cause the destabilization of the p19 dimer.

In the present work, we also investigated the influence of various salts on the equilibrium dissociation constant of CIRV p19 binding to siRNA. We observed an important decrease in affinity for 21-nt siRNA with increasing salt concentration (Figs. 2 and 3), indicative of a strong electrostatic effect. Ion pairing and hydrogen bonding interactions are considered to be dominant contributors to protein stability, particularly in dimers [36,37,40,41]. CIRV p19 forms a tail-to-tail homodimer through hydrogen bonds, hydrophobic and salt bridge interactions (between R72, R75 and R85 with E17, E35 and E41, respectively) of the two p19 monomers. Indeed, recent structural and mutational studies of the closely related TBSV p19 protein have confirmed the importance of these interactions [12,13,21]. Mutation of ionizable residues of the RNA binding cleft perturbs the electrostatic association with the sugar-phosphate backbone of the siRNA [12]. Additionally, mutational analyses of the p19 mutants P19/43 and P19/75-78 which have impaired siRNA binding activity have demonstrated the importance of ionic strength in the p19:siRNA interaction [21]. The P19/43 mutant contains a R43W substitution that is thought to interfere with hydrogen bonding to the 5′ phosphate or cause inappropriate exposure of hydrophobic residues of p19 and results in NaCl-sensitive binding to siRNA [21]. The P19/75-78 mutant contains R75G and R78G substitutions that prohibit the formation of a salt-bridge that permits the proper positioning of the caliper tryptophan residues [21]. Our observations are consistent with these previous studies and indicate that increases in ionic strength destabilize the CIRV p19:siRNA complex and that the anion effects follow the Hofmeister series [22,23]. This supports the hypothesis that the salt effect results in destabilization of the overall conformation of the p19 dimer and thus siRNA binding.

5. Conclusions

In conclusion, our results indicate that CIRV p19:siRNA interactions are affected both by pH and salt concentration. The pH dependence of CIRV p19 binding to a model 21-nt siRNA followed a pattern which suggests three important pK_a values are important in controlling CIRV p19's siRNA binding affinity. These values were extrapolated from the plot of log K_d vs. pH and are 7.1, 8.0 and 10.6. CIRV p19 contains several charged amino acid side chains, including those of histidine, cysteine and lysine, which can be assigned to the observed pK_a values. We find that the optimal siRNA binding activity of CIRV p19 occurs in the pH range from 6.2 to 7.6, although CIRV p19 still retains significant affinity for 21-nt siRNA up to pH values of 9. This suggests that salt effects are more important than pH in regulating CIRV p19:siRNA binding interactions.

Acknowledgements: The authors thank Ms. Jenny Cheng for assistance with RNA preparation. We acknowledge the Genomics and Health Initiative of the NRC for partial funding of this work. Selena M. Sagan thanks the Natural Sciences and Engineering Research Council for funding in the form of a Graduate Scholarship.

References

[1] Burgyan, J. (2006) Virus induced RNA silencing and suppression: defence and counter defence. J. Plant Pathol. 88, 233–244.
[2] Hannon, G.J. (2002) RNA interference. Nature 418, 244–251.
[3] Baulcombe, D. (2004) RNA silencing in plants. Nature 431, 356–363.
[4] Omarov, R.T., Ciomperlik, J.J. and Scholthof, H.B. (2007) RNAi-associated ssRNA-specific ribonucleases in Tombusvirus P19 mutant-infected plants and evidence for a discrete siRNA-containing effector complex. Proc. Natl. Acad. Sci. USA 104, 1714–1719.
[5] McManus, M.T. (2004) Small RNAs and immunity. Immunity 21, 747–756.
[6] Manoharan, M. (2004) RNA interference and chemically modified small interfering RNAs. Curr. Opin. Chem. Biol. 8, 570–579.
[7] Fire, A., Xu, S.Q., Montgomery, M.K., Kostas, S.A., Driver, S.E. and Mello, C.C. (1998) Potent and specific genetic interference by double-stranded RNA in *Caenorhabditis elegans*. Nature 391, 806–811.
[8] Bernstein, E., Caudy, A.A., Hammond, S.M. and Hannon, G.J. (2001) Role for a bidentate ribonuclease in the initiation step of RNA interference. Nature 409, 363–366.
[9] Elbashir, S.M., Harborth, J., Lendeckel, W., Yalcin, A., Weber, K. and Tuschl, T. (2001) Duplexes of 21-nucleotide RNAs mediate RNA interference in cultured mammalian cells. Nature 411, 494–498.
[10] Zamore, P.D. (2004) Plant RNAi: how a viral silencing suppressor inactivates siRNA. Curr. Biol. 14, R198–R200.
[11] Molnar, A., Csorba, T., Lakatos, L., Varallyay, E., Lacomme, C. and Burgyan, J. (2005) Plant virus-derived small interfering RNAs originate predominantly from highly structured single-stranded viral RNAs. J. Virol. 79, 7812–7818.
[12] Vargason, J.M., Szittya, G., Burgyan, J. and Hall, T.M.T. (2003) Size selective recognition of siRNA by an RNA silencing suppressor. Cell 115, 799–811.
[13] Ye, K.Q., Malinina, L. and Patel, D.J. (2003) Recognition of small interfering RNA by a viral suppressor of RNA silencing. Nature 426, 874–878.
[14] Lakatos, L., Szittya, G., Silhavy, D. and Burgyan, J. (2004) Molecular mechanism of RNA silencing suppression mediated by p19 protein of tombusviruses. EMBO J. 23, 876–884.
[15] Scholthof, H.B. (2006) The Tombusvirus-encoded P19: from irrelevance to elegance. Nat. Rev. Microbiol. 4, 405–411.
[16] Calabrese, J.M. and Sharp, P.A. (2006) Characterization of the short RNAs bound by the P19 suppressor of RNA silencing in mouse embryonic stem cells. RNA 12, 2092–2102.
[17] Silhavy, D., Molnar, A., Lucioli, A., Szittya, G., Hornyik, C., Tavazza, M. and Burgyan, J. (2002) A viral protein suppresses RNA silencing and binds silencing-generated, 21- to 25-nucleotide double-stranded RNAs. EMBO J. 21, 3070–3080.

[18] Sagan, S.M., Koukiekolo, R., Rodgers, E., Goto, N.K. and Pezacki, J.P. (2007) Inhibition of siRNA binding to a p19 viral suppressor of RNA silencing by cysteine alkylation. Angew. Chem. Intl. Ed. 46, 2005–2009.
[19] Mantis, N.J. and Winans, S.C. (1992) The *Agrobacterium-tumefaciens*-Vir gene transcriptional activator Virg is transcriptionally induced by acid pH and other stress stimuli. J. Bacteriol. 174, 1189–1196.
[20] Szittya, G., Silhavy, D., Molnar, A., Halvelda, Z., Lovas, A., Lakatos, L., Banfalvi, Z. and Burgyan, J. (2003) Low temperature inhibits RNA silencing-mediated defence by the control of siRNA generation. EMBO J. 22, 633–640.
[21] Omarov, R., Sparks, K., Smith, L., Zindovic, J. and Scholthof, H.B. (2006) Biological relevance of a stable biochemical interaction between the Tombusvirus-encoded P19 and short interfering RNAs. J. Virol. 80, 3000–3008.
[22] Baldwin, R.L. (1996) How Hofmeister ion interactions affect protein stability. Biophys. J. 71, 2056–2063.
[23] Collins, K.D. and Washabaugh, M.W. (1985) The Hofmeister effect and the behavior of water at interfaces. Q. Rev. Biophys. 18, 323–422.
[24] Carlson, C.B., Stephens, O.M. and Beal, P.A. (2003) Recognition of double-stranded RNA by proteins and small molecules. Biopolymers 70, 86–102.
[25] MacRae, I.J., Zhou, K.H., Li, F., Repic, A., Brooks, A.N., Cande, W.Z., Adams, P.D. and Doudna, J. (2006) Structural basis for double-stranded RNA processing by dicer. Science 311, 195–198.
[26] Johnston, D.St., Beuchle, D. and Nussleinvolhard, C. (1991) Staufen, a gene required to localize maternal RNAs in the Drosophila egg. Cell 66, 51–63.
[27] Meurs, E., Chong, K., Galabru, J., Thomas, N.S.B., Kerr, I.M., Williams, B.R.G. and Hovanessian, A.G. (1990) Molecular-cloning and characterization of the human double-stranded–RNA activated protein-kinase induced by interferon. Cell 62, 379–390.
[28] Scherly, D., Boelens, W., Vanvenrooij, W.J., Dathan, N.A., Hamm, J. and Mattaj, I.W. (1989) Identification of the RNA-binding segment of human U1 a-protein and definition of its binding-site on U1 SnRNA. EMBO J. 8, 4163–4170.
[29] Misra, V.K. and Draper, D.E. (2000) Mg2+ binding to tRNA revisited: the nonlinear Poisson–Boltzmann model. J. Mol. Biol. 299, 813–825.
[30] Chin, K., Sharp, K.A., Honig, B. and Pyle, A.M. (1999) Calculating the electrostatic properties of RNA provides new insights into molecular interactions and function. Nat. Struct. Biol. 6, 1055–1061.
[31] Ramos, A., Grunert, S., Adams, J., Micklem, D.R., Proctor, M.R., Freund, S., Bycroft, M., Johnston, D.St. and Varani, G. (2000) RNA recognition by a Staufen double-stranded RNA-binding domain. EMBO J. 19, 997–1009.
[32] Law, M.J., Linde, M.E., Chambers, E.J., Oubridge, C., Katsamba, P.S., Nilsson, L., Haworth, I.S. and Laird-Offringa, I.A. (2006) The role of positively charged amino acids and electrostatic interactions in the complex of U1A protein and U1 hairpin II RNA. Nucl. Acids Res. 34, 275–285.
[33] Ma, J.B., Ye, K.Q. and Patel, D.J. (2004) Structural basis for overhang-specific small interfering RNA recognition by the PAZ domain. Nature 429, 318–322.
[34] Song, J.J., Liu, J.D., Tolia, N.H., Schneiderman, J., Smith, S.K., Martienssen, R.A., Hannon, G.J. and Joshua-Tor, L. (2003) The crystal structure of the Argonaute2 PAZ domain reveals an RNA binding motif in RNAi effector complexes. Nat. Struct. Biol. 10, 1026–1032.
[35] Stigter, D. and Dill, K.A. (1990) Charge effects on folded and unfolded proteins. Biochemistry 29, 1262–1271.
[36] Susi, H. and Ard, J.S. (1969) Hydrophobic interactions and hydrogen bonding of caprolactam. J. Phys. Chem. 73, 2440–2441.
[37] Dill, K.A. (1990) Dominant forces in protein folding. Biochemistry 29, 7133–7155.
[38] Chu, M., Desvoyes, B., Turina, M., Noad, R. and Scholthof, H.B. (2000) Genetic dissection of tomato bushy stunt virus p19-protein-mediated host-dependent symptom induction and systemic invasion. Virology 266, 79–87.
[39] Turina, M., Omarov, R., Murphy, J.F., Bazaldua-Hernandez, C., Desvoyes, S. and Scholthof, H.B. (2003) A newly identified role for Tomato bushy stunt virus P19 in short distance spread. Mol. Plant Pathol. 4, 67–72.
[40] Klotz, I.M. and Franzen, J.S. (1962) Hydrogen bonds between model peptide groups in solution. J. Am. Chem. Soc. 84, 3461–3466.
[41] Mirsky, A.E. and Pauling, L. (1936) On the structure of native, denatured, and coagulated proteins. Proc. Natl. Acad. Sci. USA 22, 439–447.